On the Importance of Horizontal Resolution and Initial Conditions to Forecasting Tropical Intraseasonal Oscillations: the Maritime Continent Prediction Barrier

Augustin Vintzileos [1] [2] and Hua-Lu Pan [2]

[1] *Science Applications International Corporation*

[2] *Environmental Modeling Center, NOAA/NWS/NCEP*

NOAA CTB - COLA

Joint Seminar

Sep. 19, 2007

1. Introduction

There is an increasing societal need for forecast at lead times between week 3 and month 2 (e.g., Toth et al., 2007). Probabilistic information about Monsoon onsets and breaks and perhaps of heat waves and intensification/suppression of tropical storm activity could clearly benefit many sectors of the economy. The major phenomenon allowing for subseasonal forecasts is the Madden-Julian Oscillation (Madden and Julian, 1971; Zhang 2005). Subseasonal forecasting is a new challenge and as such many questions are still open or even not yet well defined. Current state-of-the-art numerical models are not representing adequately all aspects of the Tropical Intraseasonal Oscillation (TIO) in free simulations (Lin et al. 2006). Many questions are still open on effectively using dynamical models in forecast mode. How important in respect to MJO forecast is adequate initialization of these models and how far into the future can these models propagate the initial information in a useful sense? What are the sources for error growth? Can these sources be attributed to model deficiencies or to intrinsic physical reasons? Would forecast at higher horizontal resolution i.e., with improved scale interactions, be better?

Here we answer these questions using a version of the NCEP Climate Forecasting System (CFS) in a series of experiments conducted under the Climate Test Bed (CTB). After introducing a simplified measure of tropical intraseasonal oscillation activity we show that, for the CFS and for resolutions up to T254, forecast skill of the TIO is independent of horizontal resolution. The element that is crucial is atmospheric initial conditions. By ameliorating the atmospheric initial state from the Reanalysis-2 (CDAS2) to the NCEP operational analysis we improved forecast of the TIO by 3-5 days. We also show that the forecast skill of the TIO in CFS depends on the phase of the oscillation with the fastest drop in pattern correlation occurring as the convectively active phase of the MJO approaches the Maritime Continent.

2. Model and experiment description

The model that we use here is the CFS (Wang et al., 2005; Saha et al., 2006). This is a fully coupled model of the ocean-land-atmosphere system. The atmospheric component is run at three different resolutions: T62, T126 and T254 respectively 200 km X 200 km, 100 km X 100 km and 50 km X 50 km. Experiments are initialized using atmospheric initial states from both Reanalysis-2 and the operational NCEP analysis (GDAS) every five days apart from May 23 to August 11. Initial conditions from GDAS are a better representation of the state of the atmosphere as this analysis is based on the constantly improving atmospheric model, observing system and assimilation methodology. The 5-day interval between initializations is chosen because while it adequately samples Intraseasonal Oscillations can yet fit to computational limitations. In what follows we will consider experiments initialized on the following dates in 2002 to 2006: May 23 and 28, June 3, 8, 13, 18, 23 and 28, July 2, 7, 12, 17, 22 and 27 and August 1, 6 and 11. This is a total of 105 summer hindcast experiments from 2002 to 2006 (21 runs per year) for each horizontal resolution and for each initial condition which is equivalent to about 200 years of a free coupled experiment with an atmospheric model at a resolution of T126. The ocean model is used at the operational CFS resolution and initialized by the operational ocean analysis (GODAS).

Correspondence to: Augustin Vintzileos, SAIC and NOAA/NWS/NCEP/EMC
E-mail: Augustin.Vintzileos@noaa.gov

3. A measure for Tropical Intraseasonal Oscillations

There are numerous metrics for quantifying the intensity and phase of the MJO. One of the most used at present is defined in Wheeler and Hendon (2004). This index represents the coupling between the large scale circulation and organized diabatic forcing by combining winds at 200 hPa and 850 hPa and precipitation or OLR. However, in this analysis due to the constraint of a small number of years (5) which we use for computing the mean annual cycle and model drift we had to introduce a simplified version of the Wheeler and Hendon index as a measure for the MJO. This measure had to be based on a smooth field relevant to the MJO and not containing information from fields with strong variability in high frequencies like outgoing longwave radiation (OLR) or precipitation.

We construct the simplified MJO index using the observed (Reanalysis-2) 6-hourly zonal wind at 200 hPa averaged between 20ºS - 20ºN. We first compute the mean annual cycle using monthly mean data. Then we interpolate the mean annual cycle to 0, 6, 12 and 18 UTC and we subtract it from the raw data at each longitudinal grid point. Then we subtract the zonal mean at each time step and from each grid point.

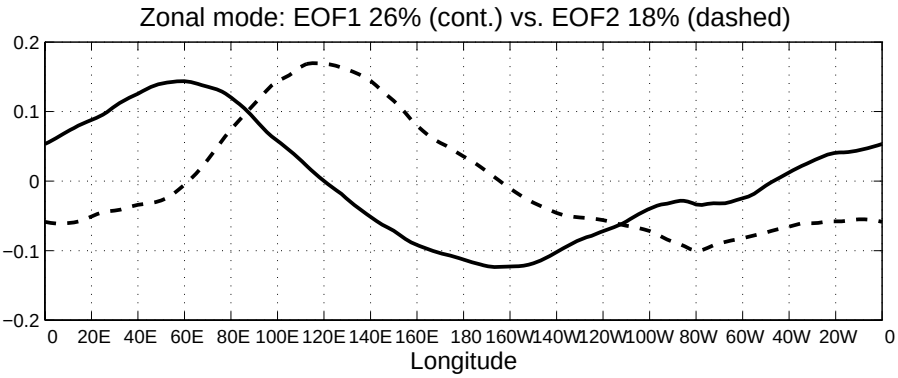

Figure 1 The first and second EOFs of the zonal wind at 200 hPa averaged 20ºS – 20ºN. Percentages of explained variance are 26% and 18% for the first and second mode respectively.

After subtracting the annual mean cycle and the zonal mean from the original data we perform an EOF analysis. It has to be noticed that no time filtering is used here. The first and second modes are shown on Figure 1. Their respective principal components (not shown) present a maximum lag correlation of 0.6 at 10 days apart with mode 1 leading mode 2. It follows that these two first modes represent an eastward propagating wave with a period of 40 days. We repeated this analysis using only winter or summer data and the resulting modes were very similar.

In the following section we use these modes in order to extract the TIO modes from the forecast and from the observations. Figure 2 compares the observed anomalies of zonal wind at 60E (thin dashed line) with the observed anomalies projected to the modes of Figure 1. It is clear that this projection method filters higher frequencies without decreasing the amplitude of intraseasonal oscillations. We therefore do not use time filtering of forecast and observed zonal wind data.

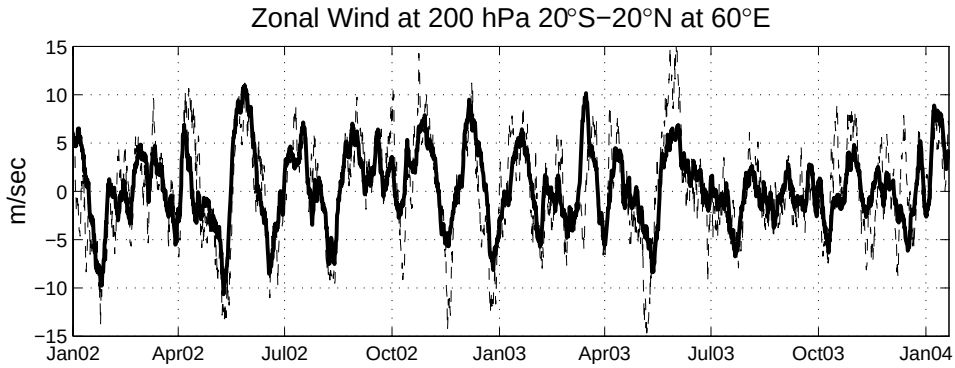

Figure 2 Zonal wind anomalies averaged between 20ºS – 20ºN at 60ºE. The thin dashed line is the observed anomalies and the thick line shows the reconstruction of the signal as projected to the first two EOF modes of Figure 1.

4. Forecast skill

The dependence of the forecast capacity of the CFS as a function of horizontal model resolution and initial conditions is shown on Figures 3 for pattern correlation and 4 for root mean square error. In both figures results for the persistence forecast is shown by the thick continuous magenta line. Black, red and blue colors correspond to resolutions of

T254, T126 and T62 respectively. Continuous/dashed lines show forecast initialized by GDAS/CDAS2. All resolutions and all initializations are more skilful than persistence forecast. Inspection of both Figures 3 and 4 shows clustering of pattern correlation and error. The separation criterion for the two clusters is initial conditions. Skill does not show any significant dependence on model resolution. The better and more compatible to the CFS initial conditions show an improvement that ranges between 3 and 5 days.

5. Reasons for the drop in forecast skill

In the previous paragraph we have shown that the anomaly correlation between the observed and forecast MJO modes is monotonically decreasing as a function of lead time. In order to understand reasons for this drop we present the pattern correlation as a function of initialization day (x-axis) and lead time (y-axis) in Figures 5 for (a) persistence forecast, (b) forecast initialized by the CDAS2 initial conditions and (c) forecast initialized by the GDAS initial conditions. Although Figures 5 present only forecasts initialized from the end of May to the beginning of August 2002 (for simplicity of the presentation) results are similar in all other initialization periods and thus the conclusions that follow can be generalized.

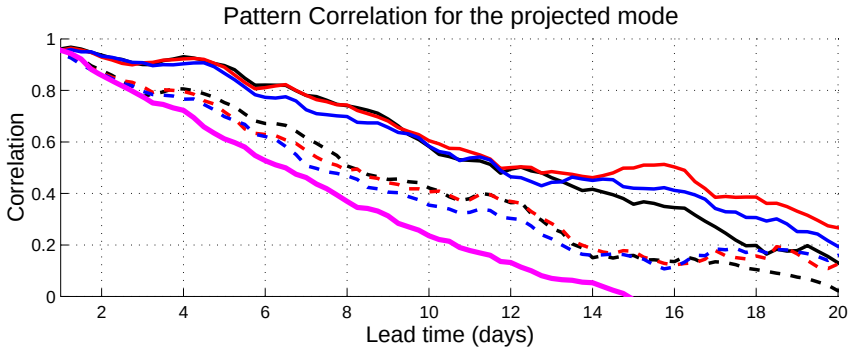

Figure 3 Pattern correlation between forecast and observations of a measure of TIO activity (see text). Model resolution is indicated by the different colors T62, T126 and T254 for respectively Blue, Red and Black. Initial conditions are indicated by dashed lines for and Black. Initial conditions are indicated by dashed lines for Reanalysis-2 and continuous lines for the operational analysis. The thick magenta line is the persistence forecast

Figure 5a shows pattern correlation obtained for a persistence forecast. Red colors represent a good forecast while dark blue colors indicate a forecast with opposite phase from the observed quantity. A good persistence forecast (vivid red colors) indicates a rather stationary pattern while a bad forecast (light red to deep blue colors) points to a progressive pattern. Increase in skill with lead time occurs due to the oscillatory behavior of the observed quantity (eventually the phase of the oscillation will reach again its values at initialization).

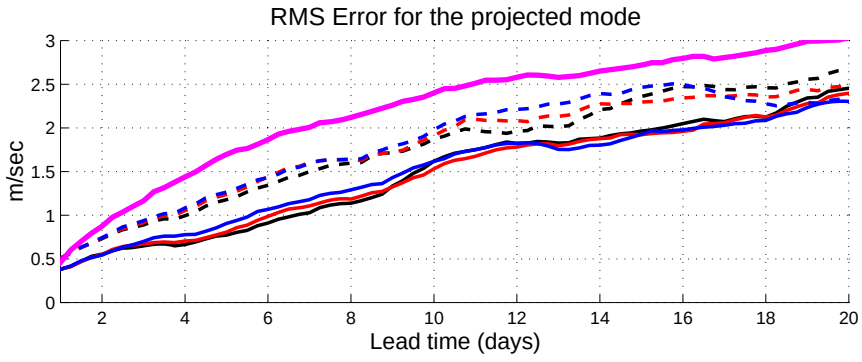

Figure 4 As in Figure 3 except for the RMS error.

In Figure 6 we show a longitude-time graph of the observed zonal velocity at 200 hPa projected to the MJO EOFs. Due to the incapacity of persistence forecast to capture changes, Figure 5a indicates that a progressive pattern exist from May to the third week of June followed by a rather stationary pattern until the beginning of August, followed by a progressive pattern in August. This succession of progressive and stationary patterns is clearly seen on the reconstructed upper troposphere MJO signal.

Figures 5b and 5c show forecast obtained with the CFS initialized by the CDAS2 and the GDAS products respectively. There is a clear improvement in forecast skill for predictions initialized after the first couple of weeks in June 2002. Inspection of Figure 6 shows that this period of improved skill coincides with the propagation of the enhanced convective phase of the MJO from the western Pacific eastwards and of the suppressed convective phase of the MJO over the Indian Ocean eastwards. However, during periods when the actively convective phase of the MJO is over the Indian Ocean and enters the Maritime Continent i.e., at the beginning of July and August (Fig. 6) there is no improvement in skill (against the persistence forecast). We define this drop in skill during the phase of the MJO when enhanced convection is over the Indian Ocean and enters the Maritime Continent as the Maritime Continent Prediction Barrier. Similar behavior has been observed in other operational forecasting systems like at ECMWF (Frederic Vitard, personal communication).

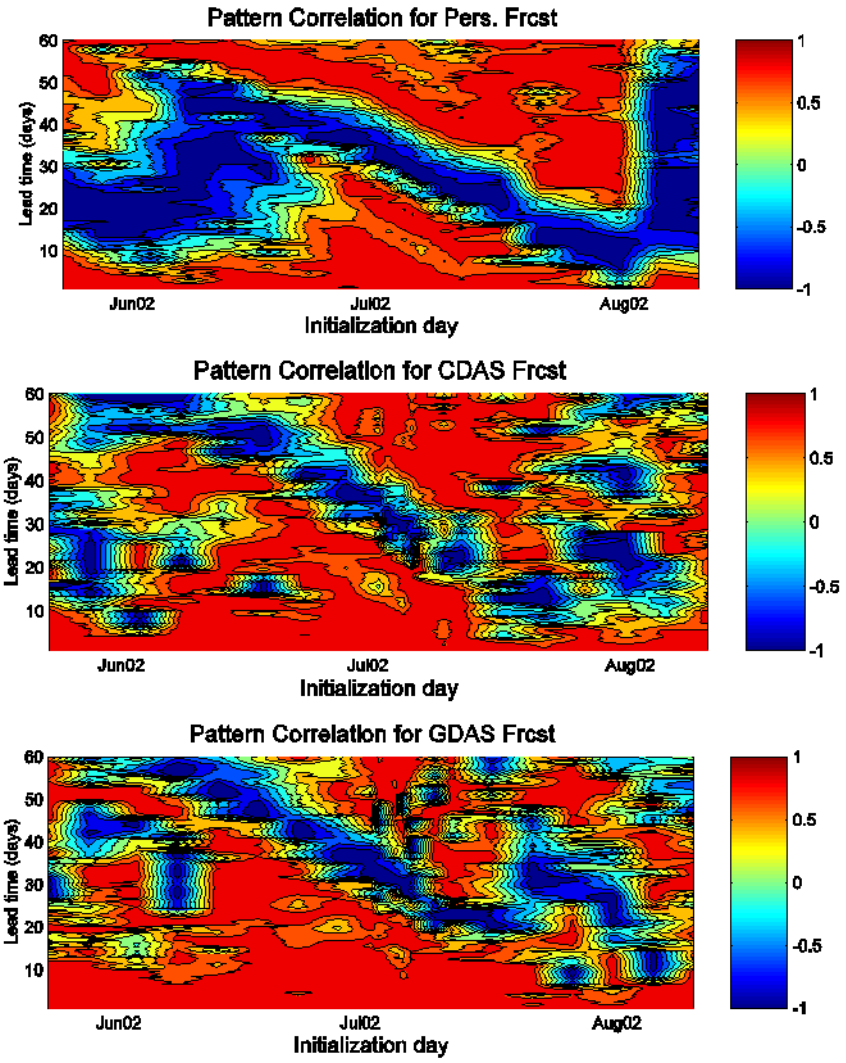

Figure 5 Pattern correlation between the EOF filtered MJO signal for forecast and observations: (a) persistence forecast, (b) CFS forecast initialized by CDAS2 and (c) CFS forecast initialized by GDAS.

6. Conclusions

We demonstrated that the CFS present a good forecast capacity of the MJO up to week 3 (for pattern correlations of 0.4) when the model is initialized by the best initial conditions available – this is a skill similar to other operational forecasting centers. In fact, improving initial conditions from the CDAS2 to GDAS improves the forecast by 3-5 days. This improvement is due to two reasons. First, the atmospheric model used in this version of the CFS is more compatible with the model used to produce GDAS than with the model used to produce CDAS2. It follows (not shown here) that initialization shocks are more important when CDAS2 initial conditions are used. Further, GDAS has a better representation of the state of the atmosphere due to additional improvements of assimilation methodologies and the observing system.

We have shown that the skill of the CFS depends on the phase of the MJO. The worst forecasts are obtained when the active convective phase of the MJO is over the Indian Ocean and enters the Maritime Continent. Despite the improvement in forecast skill of the MJO conveyed by the better initial condition we were not able to break this Maritime Continent Barrier. The fact that similar behavior was noted in other forecasting systems suggests that there is either a physical reason for this barrier or that these forecasting systems present some similar shortcomings in their design. We currently examine actively the second possibility by investigating the role of ocean initial conditions on the MJO forecast. In fact, preliminary analysis on observed fields suggest

coupling between the MJO and SST. Currently, the ocean analysis system (GODAS) which was designed and optimized for seasonal forecasting is not representing adequately periodicities relevant to the MJO. Therefore, we are now investigating an experimental version of GODAS with a more realistic behavior at subseasonal periodicities and the impact that this has on MJO forecasts.

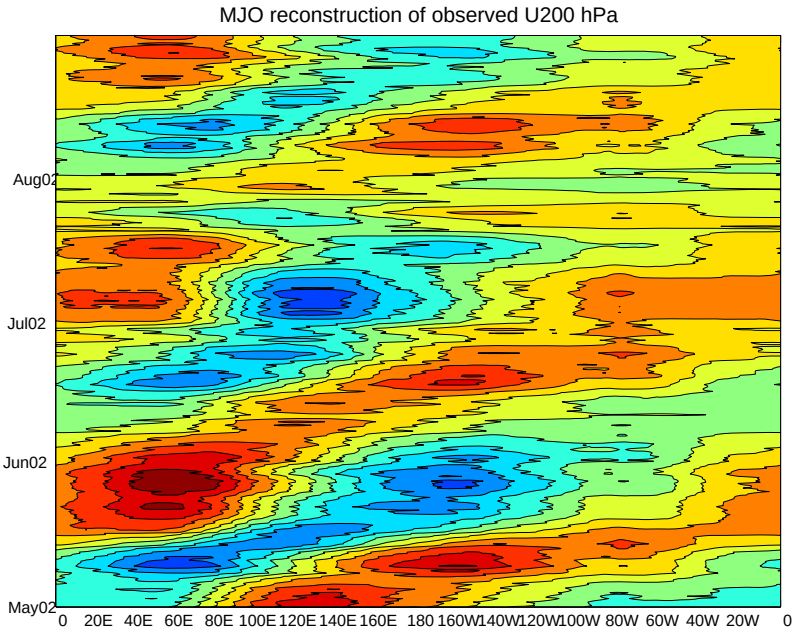

Figure 6 Longitude–time graph of the projection of the observed zonal velocity at 200 hPa averaged between 20S–20N on the two EOFs shown in Figure 1.

References

Lin, J.-L., and co-authors, 2006: Tropical Intraseasonal Variability in 14 IPCC AR4 Climate Models. Part I: Convective Signals. *J. Climate*, **19**, 2665-2690.

Madden, R. A., and P. R. Julian, 1971: Detection of a 40–50 Day Oscillation in the Zonal Wind in the Tropical Pacific. *J. Atmos. Sci.*, **28**, 702-708.

Saha, S., and co-authors, 2006: The NCEP Climate Forecast System. *J. Climate*, **19**, 3483–3517.

Toth, Z., M. Pena, and A. Vintzileos, 2007: Bridging the gap between weather and climate forecasting - Research priorities for intraseasonal prediction. *Bull. Amer. Meteor. Soc.*, **88**, 1427-1429.

Wang, W., S. Saha, H. Pan, S. Nadiga, and G. White, 2005: Simulation of ENSO in the New NCEP Coupled Forecast System Model (CFS03). *Mon. Wea. Rev.*, **133**, 1574–1593.

Wheeler, M. C., and H. H. Hendon, 2004: An All-Season Real-Time Multivariate MJO Index: Development of an Index for Monitoring and Prediction. *Mon. Wea. Rev.*, **132**, 1917-1932.

Zhang, C., 2005: The Madden Julian Oscillation. *Reviews of Geophysics*, **43**, RG2003, doi:10.1029/2004RG000158.